Journal of Building Engineering 63 (2023) 105336

Contents lists available at ScienceDirect

Journal of Building Engineering

journal homepage: www.elsevier.com/locate/jobe

Development and characterization of eco- and user-friendly grout production via mechanochemical activation of slag/rice husk ash geopolymer

Israa Sabbar Abbas [a,b,*], Mukhtar Hamid Abed [a,c,**], Hanifi Canakci [d]

[a] Department of Civil Engineering, Gaziantep University, Gaziantep, Turkey
[b] Department of Civil Engineering, Al-Qalam University College, Kirkuk, Iraq
[c] Projects Department, Al Ramadi Municipality, Anbar, Iraq
[d] Department of Civil Engineering, Hasan Kalyoncu University, Gaziantep, Turkey

ARTICLE INFO

Keywords:
Rice husk ash
Mechanochemical activation
Rheological
Bleeding capacity
Setting time
Microstructure

ABSTRACT

In this study, mechanochemical activation was used both to increase the reactivity of a one-part geopolymer during ambient curing and as an alternative activation technique to overcome the difficulties associated with conventional two-part geopolymers. The mechanochemical grinding of raw materials of varied compositions in a solid-state resulted in the synthesis of ready-to-use geopolymeric precursors, which with just the addition of water, resulted in the development of eco- and user-friendly geopolymer grout. In addition, conventionally activated geopolymer grout and ordinary Portland cement (OPC) grout were investigated for comparative purposes. Four rice husk ash (RHA) replacement ratios were used (0%, 10%, 20%, and 30% by the total precursor weight) to investigate the feasibility of using RHA as a partial precursor in slag-based mechanochemically activated geopolymer (MSG) grout. A series of tests were examined, such as rheological behavior (flow curve response, yield stress, and plastic viscosity), fresh properties (setting time and bleeding capacity), mechanical characteristics (unconfined compressive strength, ultrasonic pulse velocity), and microstructure analysis (scanning electronic microscopy, X-ray Diffraction). The experimental results showed that the rheological characteristics and fresh properties of MSG grouts were considerably enhanced in terms of groutability when slag was replaced with 0–30% RHA. In addition, the mechanical characteristics increased with the increased partial replacement of slag with RHA up to 20% and decreased beyond that. In terms of activation mechanism, the mechanochemical activation technique reduced the rheological characteristics and fresh properties while the strength increased by 18% compared to the conventional activation method. Microstructural analysis revealed the existence of more unreactive particles in both conventionally activated geopolymer and MSG grout containing 30% RHA. The results also confirmed that MSG grouts had a shorter setting time and more stable bleeding capacity than OPC grout.

* Corresponding author. Department of Civil Engineering, Gaziantep University, Gaziantep, Turkey.
** Corresponding author. Department of Civil Engineering, Gaziantep University, Gaziantep, Turkey.
E-mail addresses: israasabbar52@gmail.com (I.S. Abbas), eng.mukhtar92@gmail.com (M.H. Abed), hanifi.canakci@hku.edu.tr (H. Canakci).

https://doi.org/10.1016/j.jobe.2022.105336
Received 29 May 2022; Received in revised form 25 September 2022; Accepted 26 September 2022
Available online 7 October 2022

1. Introduction

Grouting is one of the most efficient methods for improving soil based on stability and deformation issues, filling cracks and voids to prevent water seepage, and resolving building differential settlement problems [1–4]. Grouting materials should have the advantages of low viscosity, high fluidity, high mechanical strength, low cost, and greening the environment [5]. Ordinary Portland Cement (OPC) is the most widely used construction material in contemporary construction engineering, and its annual demand is anticipated to reach 3.68–4.38 Gt by 2050 [6,7]. However, the production of OPC is associated with many environmental issues, such as the consumption of 5% of natural resources and the generation of 5–7% of total global anthropogenic carbon dioxide emissions [8–11]. These negative effects on the environment and natural resources have prompted numerous researchers to develop an environmentally friendly alternative cementitious material. Geopolymer, a three-dimensional (3D) amorphous inorganic aluminosilicate compound, is a promising material with considerable potential to be used as an OPC alternative. These geopolymers are typically produced by the geopolymerization of cost-effective aluminosilicate precursors and alkali activators, primarily alkaline hydroxide and silicate. Slag, a byproduct of pig iron production in steel plants that shows high mechanical strength and good durability in corrosive environments, is a common calcium aluminosilicate solid waste material that is widely used in geopolymer [12–17]. However, the sticky, caustic, and user-hostile activator solutions make applying the conventional (two-part) geopolymer impractical. Replacing this conventional activation method is essential to promote the widespread commercialization of geopolymeric materials because it is not a user-friendly process. The dissolving of sodium hydroxide in water is an exothermic reaction that produces a highly hazardous alkaline solution. One-part geopolymers are suggested to address several drawbacks associated with conventional (two-part) geopolymer binder designs. One-part geopolymers are synthesized using a combination of solid aluminosilicate precursors and alkaline activators. Different synthesis approaches to creating one-part geopolymer material have been proposed or reviewed [7,18–20].

Coppola et al. [21] reported that the durability resistance of one-part alkali-activated slag-based (AAS) mortars increased as the alkali content increased. Li et al. [22] investigated the rheology behaviors of one-part alkaline activated pastes prepared with a solid sodium water glass as the activator and compared them with those of OPC paste. The results showed that the plastic viscosity of the one-part alkali-activated pastes was much higher than that of OPC paste with a similar flow value, but it was also shown that the yield stress of OPC paste was much higher. Nevertheless, the studied one-part systems are commonly dominated by crystalline tectosilicates (zeolites), and the reported strength performance is typically inferior to that of conventional two-part geopolymers [20,23–26]. Ren et al. [27] studied the various properties of one-part alkali-activated slag (AAS) binders and two-part control samples. Based on the results of the one-part AAS, the hardening time was significantly prolonged and the later compressive strength was decreased (from 28 days). Additionally, less C-A-S-H gels were present, and the material was more susceptible to efflorescence. Furthermore, one-part geopolymers are almost exclusively researched in heat curing, which restricts their potential application sectors to those in which heating is not permitted (e.g., grouting, in situ building materials, rendering, restoration, etc.) [28]. Thus, mechanochemical activation is adopted in this study to enhance the reactivity of a one-part geopolymer during ambient curing and to serve as an alternative activation mechanism for overcoming the limits of traditional two-part geopolymers.

Mechanochemical activation is a method for manufacturing geopolymers via an innovative solid-state chemistry mechanism that involves co-grinding small particles of solid matter to create molecular, reactive, dense, and amorphous aggregated composite particles [29]. It requires solid binders, such as aluminosilicate source and alkaline activators, which are combined in a ball mill, and, as such, require only water to commence the geopolymerization process [30]. The intense grinding or milling process can introduce defects and electrostatic charges onto the surface of the particles, increasing the surface energy and causing crystalline to amorphous phase changes [31,32] and activated particle agglomeration [33]. Furthermore, mechanical activation can increase reactivity and improve the geopolymerization rate [34,35]. The mechanochemical approach is used in this research to ease the utilization of geopolymer materials and serve as an alternative activation technique for addressing the drawbacks of traditional geopolymer activation. Limited investigations have addressed the performance of geopolymer activated by the mechanochemical activation method. Kushwah et al. [36] developed a solid form of geopolymeric material by ball-milling aluminosilicate precursors with dry chemical activators. The geopolymeric precursors were made by initiating a reaction between an alkaline solution and alumina-silicates sources. The results indicated that the effect of ball-milling duration was significant from 2h to 6h, and the strength was considerably enhanced; however, the strength was negatively reduced when the grinding duration was higher than 6h (8, 10, and 12h). Mukhtar et al. [37] compared the rheological and mechanical properties of the mechanochemical activation method and its counterpart, conventional activation. The results demonstrated that the activation via the mechanochemistry approach significantly enhanced the mechanical properties of geopolymer grout compared to conventional activation. Hosseini et al. [30] indicated that mechanochemical activation enhanced the dispersion of bottom ash-fly ash particles, altered the Na_2SiO_3 and aluminosilicate reaction kinetics, intensified the interconnectivity of geopolymer structure, and decreased pore size; thus, the compressive strength significantly increased between 60% and 80%. Gupta et al. [29] reported that the mechanochemical reactions between fly ash precursor and NaOH in the dry state considerably improved the mechanical performance of geopolymer systems.

Previous studies only focused on fly ash and slag-based-mechanochemical geopolymer; however, other waste materials such as glass powder, rice husk ash, metakaolin, etc. remain unexplored. Therefore, this study focuses on the influence of rice husk ash replacement on the performance of mechanochemically activated slag-based geopolymer grout. Mukhtar et al. [23] examined the effect of mechanochemical activation on the rheological parameters of a one-part geopolymer grout. The results revealed that the initial apparent viscosity of mechanochemical activation of one-part geopolymer grout was approximately 59% higher than that of samples of one-part geopolymer grout under identical conditions. Wang et al. [38] also reported that the workability and fluidity of one-part fly ash/slag-based geopolymer were improved through mechanical activation.

Rice husk is an abundantly available agro-waste product, with an annual worldwide output of 70 million tons [39,40]. Rice husk

ash (RHA) is produced by the controlled incineration of rice hulls and consists of 85–95 wt% amorphous silica [20,39]. The improper disposal of RHA generates several environmental issues, such as the formation of ash lands, air pollution, and water contamination, all of which are hazardous to human health [41–43]. Therefore, it should be a priority to find sustainable solutions to use this ash rather than dispose of it in landfills. In the previous decade, various research has been conducted to employ RHA as a supplemental component of OPC or sand for mortar or concrete as a silica source, filler material, and precursor in geopolymers [44]. Meja et al. [45] assessed the feasibility of using an agro-industrial byproduct, RHA, as a replacement for commercial sodium silicate. The results showed that the RHA may be used to produce alkali-activated materials with 42 MPa at 7 days. The study also confirmed that both amorphous silica and a portion of the crystalline silica included in RHA participate in the alkaline activation process provided that the alkalinity is attentively controlled. Luukkonen et al. [46] investigated whether fast-dissolving solid synthetic sodium metasilicate could be substituted with sodium hydroxide and slow-dissolving silica produced from RHA in the preparation of alkali-activated slag mortar. The results indicated that the availability of silica considerably influences the development of compressive strength as a function of time or mixture composition.

Liang et al. [47] examined the strength development, thermal stability, and microstructures of metakaolin-RHA based geopolymers in which RHA partially replaced metakaolin up to 40%. The findings showed that RHA particles worked as pore-fillers, hence enriching gel phases, which exhibited superior thermal stability compared to OPC paste. Zhu et al. [48] studied the effect of RHA content on the waterproofing and microstructural characteristics of an ultrafine fly ash-based geopolymer. These results highlighted how the specific honeycomb-hole influence and active silicon oxide brought by rice husk ash result in the structure densification and decrease the presence of calcium hydroxide and contribute to the creation of gel, which would significantly lead to the enhancement of the waterproofing property. Sturm et al. [20] created one-part geopolymers from RHA and sodium aluminate. The results reveal that RHA is highly reactive and can produce an exemplary geopolymer gel with higher compressive strength than is typically observed for one-part geopolymers. Celik and Canakci [49] studied the fluidity and rheological characteristics of cement-based grout combined with RHA. The test findings demonstrated that increasing the RHA replacement rate increases plate cohesion, plastic and apparent viscosity, marsh cone flow time, and yield stress while decreasing the diameter of the mini-slump. Istuque et al. [50] assessed the compressive strength performance of alkali-activated mortars, finding that using RHA as a silica source to generate sodium silicate suspensions which are then utilized as chemical activators conferred greater sustainability to these systems.

The current research aimed to develop mechanochemically activated geopolymeric grout with an environmentally and more user-friendly approach. Current geopolymer synthesis methods primarily address the limitations of conventional geopolymerization techniques. In addition, in this study the effects of RHA replacement on the performance of mechanochemical geopolymer grout were also investigated. Rheological properties (flow curve response, yield stress, and plastic viscosity), fresh characteristics (setting time and bleeding capacity), mechanical characteristics (unconfined compressive strength, ultrasonic pulse velocity), and microstructure analysis (scanning electronic microscopy) were tested for all the examined types of grouts.

2. Experimental work

2.1. Materials

This study used slag and rice husk ash (RHA) to produce the mechanochemical geopolymer. The slag is procured from the iron and steel industry (Iskenderun Iron and Steel Plant in Hatay province-Turkey), and the RHA is obtained as commercial waste material from a rice manufacturing factory in Edirne, Turkey. RHA is produced by burning rice husks at temperatures between 500 and 600 °C. The RHA that passes through the 150 μm sieve was adapted for mechanochemical activation. Also, CEM I-42.5R Portland cement per ASTM C150 was used to produce Portland cement grout for comparison purposes. The alkaline activators utilized in this investigation were sodium hydroxide (98% purity) and sodium silicate, both of which were purchased from AS Kimya Co, (İstanbul, Turkey). The ratio of sodium metasilicate powder (Na_2SiO_3-Penta) to sodium hydroxide is 0.5. Table 1 summarizes the physical and chemical properties

Table 1
Physical and chemical properties of OPC, slag, RHA, and Na_2SiO_3.

Constituent (%)	OPC	Slag	RHA	(Na_2SiO_3-Penta) Powder
a) Chemical composition				
CaO	62.58	34.19	1.38	
Al_2O_3	5.31	10.6	0.1	
SiO_2	20.25	40.42	91.6	28
Fe_2O_3	4.04	1.28	0.64	
MgO	2.82	7.63	–	
SO_3	2.73	0.68	0.21	
K_2O	0.92	0.0128	5.14	
Na_2O	0.22		–	29
Loss on ignition	4.4	–	5.43	–
Modulus ratio				1
H_2O				43
b) Physical properties				
Specific gravity	3.15	2.9	1.97	
Specific surface (m^2/kg)	326	565	1060	

characteristics of the OPC, precursor components (slag and RHA), and Na_2SiO_3.

2.2. Mechanochemical geopolymer preparation

In this study, the mechanochemical activation (co-grinding NaOH, sodium metasilicate, slag, and RHA for 2 h) was carried out in an 80 kg ball mill equipped with 12 balls with a diameter of 45 mm and a mass of 400 g. During the co-grinding process, the particles of source materials are trapped between the balls and chamber walls and subjected to continuous impact and milling; the collision between the tiny rigid balls in a container generates localized high pressure. This results in a decrease in particle size, an increase in specific surface area, a decrease in crystallinity, a change in the mineralogical composition, and an increase in the amorphous phase. After that, the obtained geopolymeric precursors are mixed with faucet water to create MSG grout. It is worth noting that the grinding period for the geopolymeric precursors was set at 2 h based on previous studies [28,36,37,51]. In this study, the specimens' names (RH0-MSG, RH10-MSG, RH20-MSG, and RH30-MSG) are denoted with specific codes. The labels RH and MSG represent rice husk ash and mechanochemically activated slag-based geopolymer, respectively, and the numbers'0,' '10,' '20,' and '30' indicate the percentage of rice husk ash content in the slag-based mechanochemically activated geopolymer by weight. For comparison, conventionally activated slag-based geopolymer (CSG) grout (to examine the effect of the activation method) and ordinary Portland cement grout were prepared.

Regarding CSG preparations, NaOH beads were calculated and weighed at a molarity of 3.75 and dissolved in faucet water. An exothermic reaction occurred during the mixing time, and the NaOH solution became extremely hot. Because of this, the liquid was kept at room temperature before use until chemical equilibrium was achieved; after the sodium hydroxide liquid cooled down, the Na_2SiO_3 was added. In general, the alkali activator solution was prepared at least one day before mixing the CSG ingredients. The alkali solution was then mixed with slag to synthesize CSG grout. Also, OPC was mixed with water (the same water amount used to prepare MSG grout at 3.75 M) to produce OPC grout for comparison purposes. The mix proportions of all studied mixes are summarized in Table 2.

2.3. Testing methods

All grout mixtures were prepared in the laboratory at a temperature of 23 ± 3 °C. Rheological experiments were conducted in accordance with [52] utilizing a rational viscometer (proRheo R .180). The grout mixtures were unable to produce flow responses at shear rates less than $500s^{-1}$ during the viscometer trials. Thus, shear rates ranging from $500s^{-1}$–$1000s^{-1}$ (Fig. 1) were used to investigate the flow responses of shear stress and apparent viscosity of grout [53–55]. All shear rates were maintained for a duration of 15s in order to achieve an equilibrium condition in a total of 120s for each mixture.

The flow curves of shear stress and apparent viscosity vs. shear rate were determined for both portions (descending and ascending). Markedly, the ascending portion of data was considered in this research since their trend lines correspond to an undisturbed condition [56–59]. In the rheological curves of nonlinear response, the dilatant (shear-thickening) behavior appears when the viscosity increases as the shear rate rises. In contrast, if viscosity decreases as the shear rate build, the flow exhibits pseudoplastic (shear-thinning) behavior [57]. In this research, a modified Bingham model was used to determine the yield stress and plastic viscosity based on previous investigations [56,57,60], as described in Eq (1):

$$\tau = \tau_0 + \mu_p \dot{\gamma} + c\dot{\gamma}^2 \quad (1)$$

Where, τ is shear stress (Pa), τ_0 is the yield stress (Pa), μ_p is the plastic viscosity (Pa.s), and C is a constant. In the modified Bingham model, the ratio of the second-order term to the linear term could be used to characterize a nonlinear response, indicating shear thickening, shear-thinning, and the Bingham model for $C > 0$, $C < 0$, and $C = 0$, respectively [61–63].

Regarding fresh properties, the setting time was measured by conducting Vicat needle tests in accordance with ASTM C191-19 [64] recommendations. According to ASTM C940-16 [65], bleeding capacity tests were conducted to show the grout stability. The fresh grout was placed in a 1000 mL graduated cylinder for 120 min. The volume of bleed water was then measured every 30 min till the end of the observation period.

Table 2
Mix proportions of grout.

Mix ID	Weight: %						Weight: (g)					
	Slag %	RHA %	NaOH %	OPC %	Na_2SiO_3%	Grinding duration:h	Slag (g)	RHA (g)	NaOH (g)	Na_2SiO_3 (g)	OPC (g)	Water (g)
RH0-MSG	85	0	10	–	5	2	850	0	100	50	–	750
RH10-MSG	75	10	10	–	5	2	750	100	100	50	–	750
RH20-MSG	65	20	10	–	5	2	650	200	100	50	–	750
RH30-MSG	55	30	10	–	5	2	550	300	100	50	–	750
CSG	85	0	10	–	5	-	850	0	100	50	–	750
OPC	-	-	-	100	–	-	–	-	-	-	1000	750

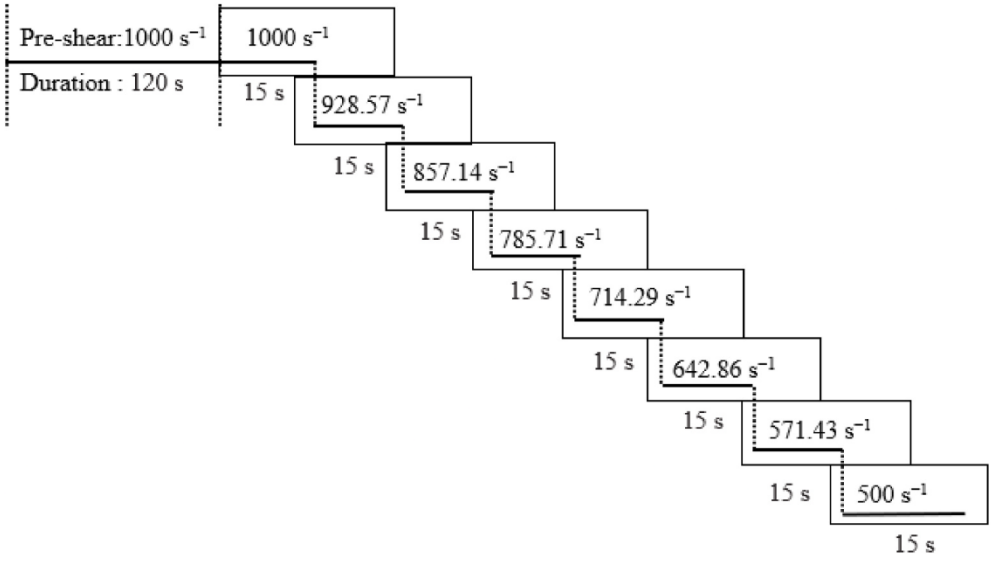

Fig. 1. The shear rate protocol was used to draw the flow curves.

In order to obtain mechanical characteristics, the fresh grout was cast into cylindrical molds with a height of 100 mm and diameter of 50 mm to examine the unconfined compressive strength (UCS) for geopolymer grouts in accordance with standards [66,67]. The grout specimens were kept at room temperature for 7 days and 28 days. Before conducting the UCS tests, the samples were utilized to determine the wave velocity using ultrasonic pulse velocity (UPV) [68]. The magnitude of UPV measurements can be interpreted by some categorizations given in past work [69] (Table 3). The bulk density of grout specimens was also estimated during the testing. The bulk density measurement was obtained by measuring the mass and dimension of the samples. The Particle size distribution was evaluated using a Malvern Mastersizer 2000 laser particle size analyzer. This test was conducted on raw RHA and slag, in addition to co-grinding RHA and slag with solid chemicals (sodium hydroxide and sodium metasilicate). A ZEISS Gemini SEM 300 was used to perform a scanning electron microscopy (SEM) examination on raw RHA and slag powder, as well as co-grinding RHA and slag with solid chemicals, in order to examine the changes in the microstructure caused by the mechanochemical activation mechanism. After 28 days, SEM analysis was also conducted on hardened geopolymer grouts (MSG and CSG) to assess the influence of the activation method and RHA substitution. The samples for SEM analysis were taken from the broken particles of the specimens which were tested under UCS and then covered with gold coatings for accurate SEM imaging. The sample sizes were around 20 mm in diameter and 10 mm in height. X-ray diffraction (XRD) was employed to qualitatively assess the crystalline structure of each geopolymeric precursor before and after mechanochemical activation and hardened geopolymer grout.

3. Results and discussions

3.1. Particles size analysis

The particle size is considered the primary factor controlling rheological and mechanical characteristics variance. The particle size distribution of RHA and slag before and after mechanochemical activation is shown in Fig. 2. The d50 (mean size) of raw RHA and slag was 34 μm and 22 μm, respectively, whereas the mean size of RHA and slag diminished to 23 μm and 15 μm, respectively, after 2 h of grinding in a ball mill with sodium hydroxide and sodium metasilicate, as shown in Fig. 2.

Scanning electron microscopy analysis (SEM) shows the microstructural approximation of slag and RHA precursors before and after mechanochemical activation. As shown in Fig. 3a, the raw slag particles are non-uniform and heterogeneous, with sub-rounded to angular forms for the material components. The roughness and edges were observed in both the angular and bulk particles [70]. As shown in Fig. 3b, most raw RHA particles have an irregular shape, are amorphous, and have high porosity.

Fig. 3c and d shows the microstructural analysis of the mechanochemical activation of slag and RHA precursors obtained after 2h of co-grinding in the presence of chemical powder (NaOH and sodium metasilicate). After co-grinding, the slag and RHA particles were coated with solid chemical powder (NaOH and Na_2SiO_3), which also reduced the average size of the precursors and solid chemicals (Fig. 3c and d). Nonetheless, the slag and RHA particles still develop angular and slightly deformed shapes after mechanochemical grinding. Furthermore, the surface area of the particles clearly increased during mechanochemical activation and resulted in a higher

Table 3
UPV classification [69].

UPV (m/s)	<2500	2500–3500	3500–4000	4000–5000	>5000
Definition	Very low velocity	Low velocity	Middle velocity	High velocity	Very high velocity

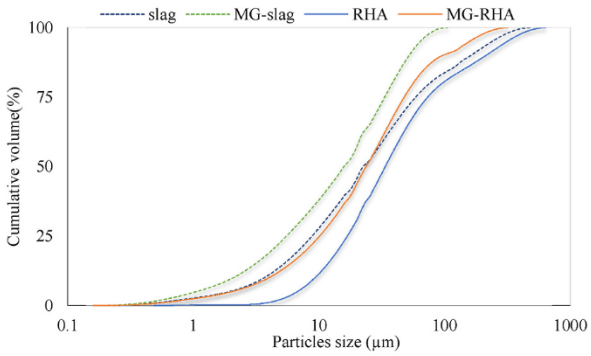

Fig. 2. Particle size distribution of RHA and slag before and after mechanochemical activation.

reaction rate of the geopolymeric precursors. Additionally, initial bonding between the particles was observed (Fig. 3d) due to the addition of NaOH and sodium metasilicate, which might reflect the MSG powder's adhesive nature. However, the influence of ball milling of all raw materials resulted in increased amorphousness and formation of the geopolymeric precursor [29]. Mukhtar et al. [37] reported that grinding of fly ash and slag with NaOH and sodium metasilicate for 2 h resulted in the formation of cracks and defects, which augmented the surface roughness of the surface the particles and conferred increased reactivity to the geopolymeric precursors.

The XRD patterns have been adopted to assess the effect of co-grinding of geopolymeric precursors before and after mechanochemical activation, as presented in Fig. 4. Before co-grinding, the raw slag-based geopolymer (RH0-SG) precursor has a vitreous structure with an amorphous nature as eminent from a hump around 28°–33° (2θ value) with a peak position at 30°. Also, crystalline phases are represented in Fig. 4 by sharp peaks composed primarily of akermanite, gehlenite, calcium silicate, and merwinite, as seen by the steep peaks reported between $2\theta = 15°$ and $2\theta = 90°$ [71,72]. After co-grinding, the peak intensity of the co-grinded RH0-MSG precursor is more attenuated than the raw RH0-SG precursor (Fig. 4), implying that the crystalline phases of the slag have amorphized as a result of the mechanochemical grinding with NaOH and sodium metasilicate. The mechanochemical activation increased the disorder and surface area and stimulated the reaction between the raw powders [29].

3.2. Rheological behavior and responses

The flow curves of grout mixes are shown in Fig. 5. Also, the dilatant index values (i.e. coefficient C) are summarized in Table 4. All the grout mixtures exhibited a shear thickening behavior ($C > 0$). In other words, apparent viscosity increased with the rise in the shear rate of grout, as illustrated in Fig. 5.

The experimental results showed that the substitution of slag with RHA considerably affected the rheological behavior of MSG grout. As shown in Fig. 5, the shear stress and apparent viscosity of MSG grout reduced as the RHA content increased. This behavior is most likely caused by the presence of active silicon oxide particles and the loose layer structure of RHA [73]. The SiO_2 particles were dissolved from the layered pore channels in RHA at the alkali activator environment, resulting in more SiO_2 micro-particles and empty pore channels emerging. The pore channels provided a space for the occupation and hydration of fine slag particles and the dissolved SiO_2 micro-particles acted as a filler for the whole pastes while participating in the reaction. The mutual-penetration effect sustained under the combined action of the pore channel and the secondary filling effect was the primary cause for the refinement of pore structure, resulting in a decrease in cumulative pore volume in the geopolymer grout [73,74]. As a result, a greater amount of water is available for lubrication, which reduces the viscosity of the MSG mix. Meanwhile, the addition of RHA dramatically affected the rheological behavior by increasing the SiO_2/Al_2O_3 ratio. According to Dadsetan et al. [75], increased SiO_2/Al_2O_3 ratios led to a reduction in shear stress and apparent viscosity of geopolymer pastes. It might be due to the slower dissolution of Si and Al monomers at ambient temperature [76]. Accordingly, Chouhan et al. [77] used RHA to develop a novel superplasticizer to address the workability issue and reduce the viscosity of the geopolymeric binder.

In terms of geopolymer activation mechanism, the apparent viscosity and shear stress of CSG grout were higher than MSG grout; it can be concluded that CSG grout mixtures mostly appear to produce higher magnitudes of apparent viscosity and shear stress in comparison to MSG grout due to the high dissolution and ionization degree of MSG grout [78]. Mukhtar et al. [37] obtained similar findings and reported that when mechanochemically activated geopolymer precursors were mixed with water, the mobility of ions and electrical conductivity of the mechanochemically activated geopolymer grout increased, leading to an increase in the degree of dissolution in the solution followed by a decrease in the solution's viscosity and degree of ion hydration. Also, the magnitudes of shear stress and apparent viscosity of the MSG grout were higher than those of the OPC grout, as illustrated in Fig. 5. This could be due to the fact that the mechanochemical process alters the surface area and particle size of the powder; as a result, additional water is required to cover the surface of the particles, resulting in a notable reduction in the amount of excess water in fresh grout and an increase in responses (shear stress and apparent viscosity) [79].

3.2.1. Yield stress and plastic viscosity

The yield stress (YS) and plastic viscosity (PV) of grout types were estimated using the modified Bingham model during rheological experiments. The YS and PV of the MSG grout gradually decreased with increasing RHA content (Table 4). The results showed that

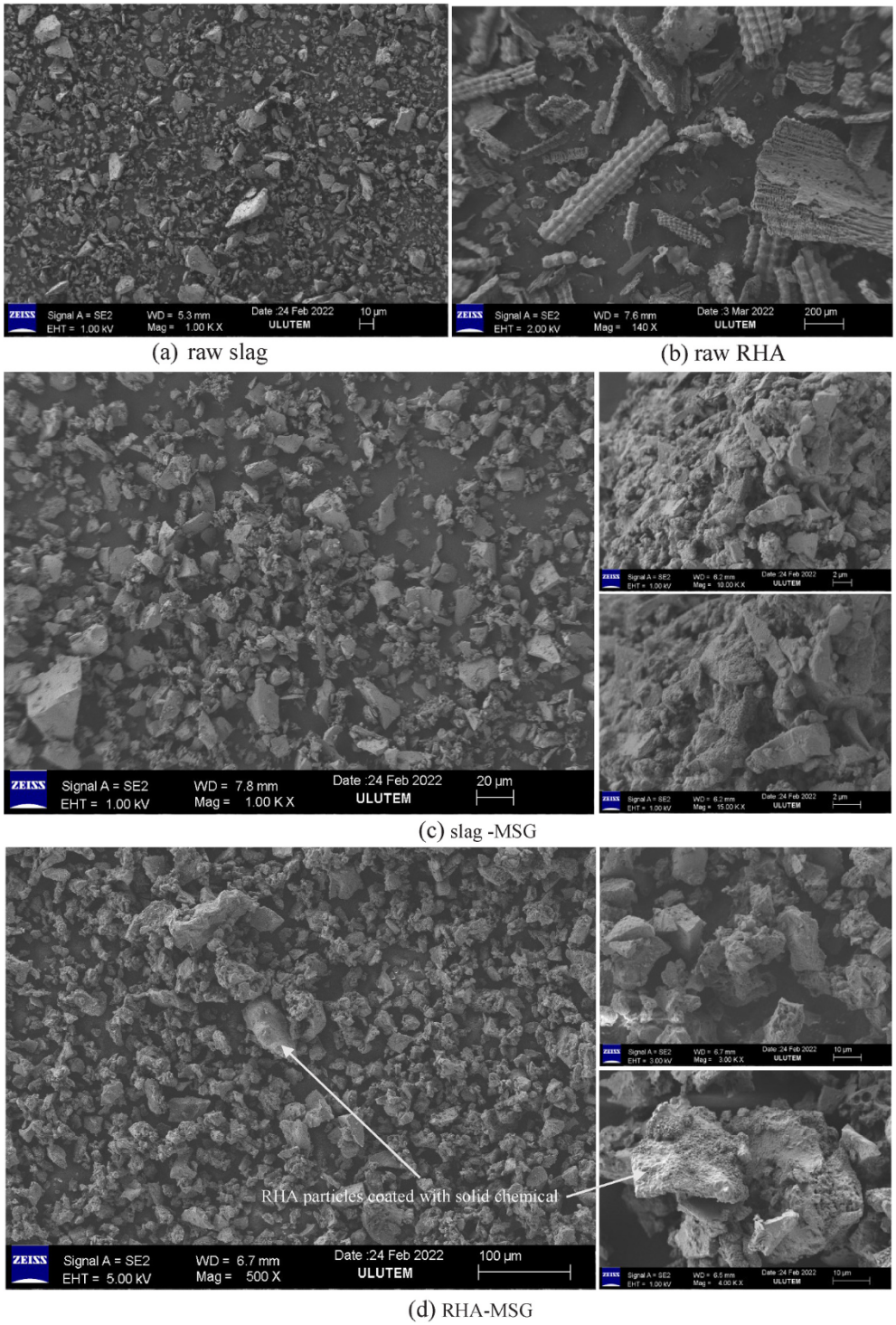

Fig. 3. SEM micrographs of (a) raw slag, (b) raw RHA, (c) slag -MSG, and (d) RHA- MSG.

mixtures with 100% slag (RH0- MSG) have higher YS and PV of 5.8 pa and 0.038 Pa.s, respectively (Fig. 6). The high values of both YS and PV of RH0-MSG are attributable to the influence of particle shape and size, which control the rheological properties of the material [80,81] as well as the accelerated chemical reaction caused by the high slag level, resulting in the creation of sodium aluminate -silicate-hydrate alongside calcium aluminate-silicate-hydrate gels at an early stage [82]. Furthermore, the increased solidification rate could arise from the accelerated formation of specific reactions in the mixed materials due to the release of the Ca^{2+} ions from the slag

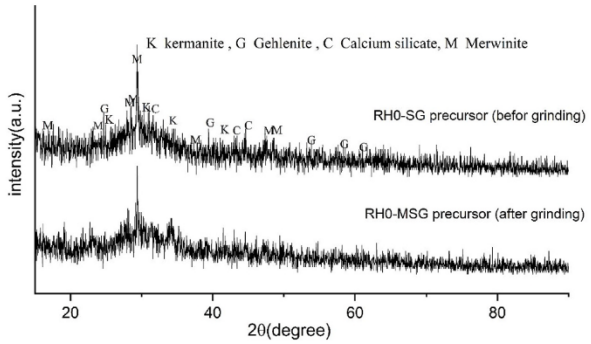

Fig. 4. XRD patterns of geopolymeric precursors before and after mechanochemical activation.

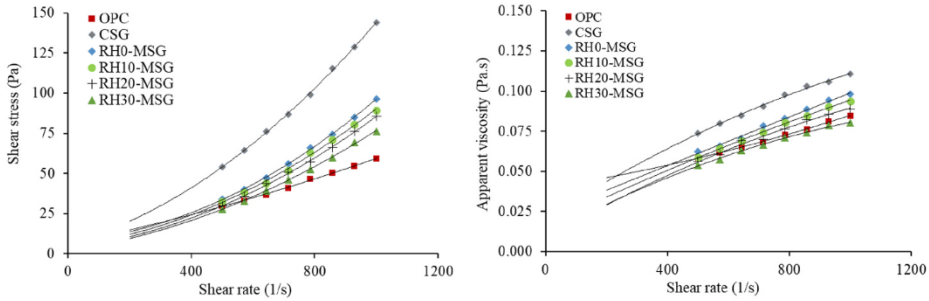

Fig. 5. Shear stress and apparent viscosity versus shear rate curves of OPC, CSG, and MSG grout.

Table 4
Rheological characteristics of the grout.

Mix ID	coefficient C	YS(Pa)	PV (Pa. s)
RH0-MSG	0.00004	5.8	0.038
RH10-MSG	0.00004	5.54	0.035
RH20-MSG	0.00004	4.76	0.03
RH30-MSG	0.00004	4.2	0.027
CSG	0.00008	6.04	0.052
OPC	0.00003	6.4	0.06

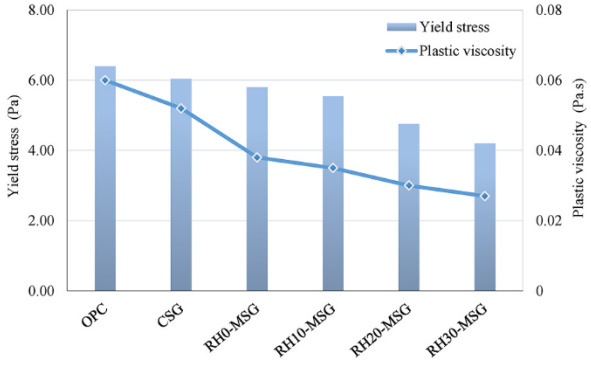

Fig. 6. YS and PV of OPC, CSG, and MSG grout.

reacting with silicates and aluminates [83,84]. Also, the incorporation of RHA into MSG grout dramatically alters the reaction products and physicochemical interactions. The YS of RH10-MSG, RH20- MSG, and RH30- MSG grouts was reduced by 5%, 22%, and 38%, and the PV was reduced by 9%, 27%, and 41% when compared to RH0-MSG, respectively. The presence of RHA promotes the filling of micropores and the formation of more amorphous gel phases, resulting in a dense structure with a low water absorption value [74].

Consequently, more water is available for lubrication, which decreases the MSG mix's viscosity.

The results also demonstrated that the YS and PV of the OPC grout were higher than those of the MSG and CSG grout, as shown in Table 4. The YS and PV of RH0-MSG grout are 5.8 Pa and 0.038 Pa s, respectively. In contrast, OPC grout has a YS and PV of 6.4 Pa and 0.06 Pa.s (Fig. 6) because cement particles begin to dissolve and hydrate upon contact with water, creating positive and negative charges on the cement surface and inducing electrostatic attraction between the cement particles, which causes grouping or flocculation of the particles [85]. In the synthetic pore solution (liquid phase of hydrating cement suspension), the hydration product ettringite was negatively charged, whereas the calcium silicate hydrates and tricalcium silicate were positively charged [86]. Liang et al. [87] reported that part of the water is wrapped in cement particles; therefore, a decrease in the amount of free water would be observed, increasing the effective solids volume fraction. However, in the MSG grout, the silicate anions are absorbed on the surface of precursor particles like slag, generating negative charges on the particles' surfaces and resulting in electrostatic repulsion between them [88]. In other words, it had a reduced effective solid volume fraction, which resulted in lower YS and PV.

From the perspective of the activation method, the MSG grout unveiled a lower YS and PV than the CSG grout (Table 4). The YS and PV of MSG grout are 4% and 27% less than the CSG grout. This could be because the alkali activator solution dissolves rapidly at an early stage when blended with the raw materials that are rich in alumina and silica to produce a conventional geopolymerization reaction, one which is significantly more viscous than the required water to form MSG grout, resulting in a greater YS and PV of the CSG grout [37]. It is well known that a suspension's viscosity increases in direct proportion to the viscosity of the suspending solution [89]. It can be concluded that the higher YS and PV values are disadvantageous for grout when used as a soil injection material, as the materials would be difficult to pump through the pipe if the slurry was overly viscous. Hence, MSG grout is more suitable for soil injection applications than CSG and OPC grout.

3.3. Fresh properties

Grouting is one of the important civil engineering applications. The setting time is an essential factor for grouting applications, where a short setting time might cause damage to the grouting machine but a long setting time often leads to a slow construction schedule [37]. The effect of RHA content on the setting times of MSG grouts is depicted in Fig. 7a. In general, the incorporation of RHA into the geopolymer composition prolonged the setting time. The initial setting time of RH10-MSG, RH20-MSG, and RH30-MSG increased by 14%, 27%, and 44%, respectively. Similarly, the final setting time increased by 6%, 16%, and 42%, respectively, compared to the control mix (RH0-MSG). This is probably due to the combined effect of biogenic active silicon oxide particles and loose-layer structure of RHA; the dissolution of silicon oxide particles from the layer structure is slow, which delays the hydration of the geopolymer [73]. Furthermore, the rate of condensation between aluminosilicate species is faster than the condensation rate between silicate-silicate species [90]. Meanwhile, the inclusion of RHA increased the SiO_2/Al_2O_3 ratio, delaying the setting time. According to Billong et al. [91], the RHA in pastes acted as a setting retarder due to the high SiO_2/Al_2O_3 ratio in the mixture, and this contributed to the inhibition of the geopolymerization reaction by the precipitation of Si–Al phases which prevented contact between the reactive material and the activation solution. Liang et al. [92] observed that the addition of RHA to the metakaolin-based geopolymer significantly prolonged the setting time, but this effect was likely attributable to the increased time required for silicon oxide to dissolve from RHA.

On the other hand, the results demonstrated that the setting time of the RH0- MSG grout was shorter than that of the OPC and CSG grouts. The initial setting time of MSG, CSG, and OPC was 3.3h, 4h, and 8h, and the final setting time was 4.5h, 6.3h, and 12h, respectively, as seen in Fig. 7a. The shorter setting time of RH0- MSG grout might be related to mechanochemical mechanisms that create electronic charges on the surface of mechanochemically activated particles, resulting in a rise in surface energy and the transition from the crystalline to amorphous phase [30]. Furthermore, the mechanochemical process disintegrates large alumina and silica particles, increasing their surface area and resulting in a more uniform distribution of particles in the mixture, and this contributed to a higher proportion of additional aluminosilicate being formed from slag and RHA, allowing for participation and

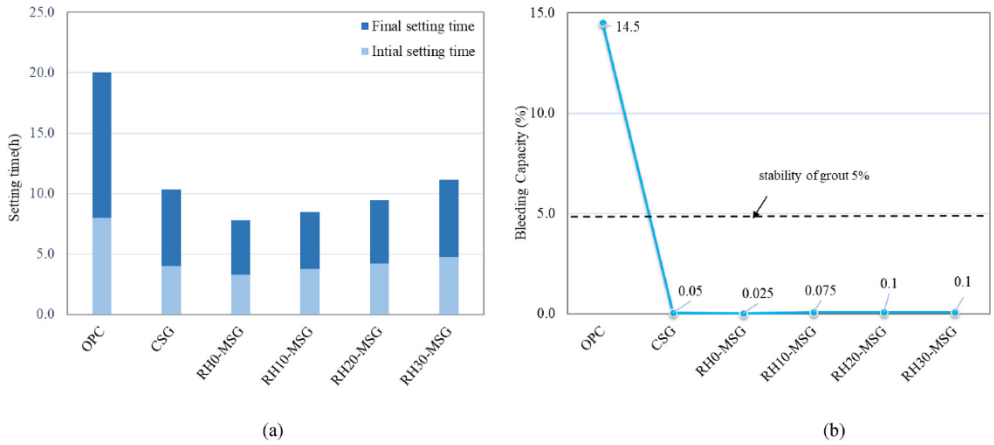

Fig. 7. Fresh properties of MSG, CSG, and OPC grout, (a) setting time, and (b) bleeding capacity.

dissolution in the formation of geopolymer gels [37,79]. Thus, increased aluminosilicate availability accelerated the polymerization process, resulting in a shorter setting time for RH0- MSG grout [79,93].

In addition, bleeding capacity testing was carried out in this work to assess the influence of RHA content on the stability of MSG grout, as shown in Fig. 7b. The results revealed that the bleeding capacity of MSG grout rose along with the increase in RHA level; hence, it can be clearly observed that the mixes with 100% slag content had the lowest bleeding capability. For example, the bleeding capacity of MSG grout rises from 0.025% to 0.1% when RHA content is increased from 0 to 30%. Because of the high demand for water in the geopolymerization of slag particles [94,95], dissolution heat flow climbed as slag amount increased since slag possesses a faster dissolution rate than RHA [88], leading to rapid growth synthesis of reaction products to create a rigid network. The heightened bleeding capacity of geopolymer grout containing RHA can be attributed to its low water demand and its filling effect compared to slag. Furthermore, the porous and reactive silica-containing RHA enhances ion transport mobility early on and precipitates the dissolving process of aluminosilicate precursors, leading to polycondensation reactions. The RHA contributes to the filling of micropores through its filling effect and imparts more amorphous gel phases, resulting in a dense structure and a lower water absorption value. The results also showed that the MSG grout (RH0-MSG) had significantly less bleeding capacity than the OPC and CSG grouts, as seen in Fig. 7b. Due to the increased surface area and reduced particle size of the mechanochemically activated powder, additional water is required to cover the surfaces of the particles [79]. Overall, the results of this research indicated that the bleeding of MSG and CSG grouts is more stable than OPC grout.

3.4. Mechanical properties

3.4.1. Unconfined compressive strength (UCS)

The UCS results of mechanochemically activated slag-based geopolymer (MSG) grout incorporating RHA were obtained at 7 and 28 days, as shown in Fig. 8. The UCS values of all studied mixtures improved as the age increased from 7 to 28 days due to the completion of the polymerization process and densification of the microstructure at longer ages [94,96,97]. On the other hand, the UCS results for MSG grout samples containing RHA revealed that the UCS rises in conjunction with curing time, and less cracks on the surface of the specimens were observed when compared to the RH0-MSG sample. However, the UCS test results of the MSG grout reduced with increasing RHA replacement content at 7 days then rises as RHA content expands at 28 days, as shown in Fig. 8. For instance, at 7 days, the reductions of UCS were 4%, 12%, and 29% for the RHA contents of 10%, 20%, and 30%, respectively. Similar results were reported in previous research [96,98]. The increase in UCS of RH-MSG grout over time is related to the dissolution of a considerable amount of silica from RHA in an alkaline environment [99]. From the perspective of geopolymers containing varying amounts of RHA, RHA contributed favorably to the development of strength. The UCS of MSG grout rose with increased partial replacement of slag with RHA up to 20% and declined beyond that. For instance, the addition of RHA as slag replacement at 10 and 20% elevated UCS values by 4.5% and 41%, respectively, compared to the control mix (RH0-MSG) at 28 days. The increased UCS with the addition of RHA is due to the relatively higher SiO_2/Al_2O_3 ratio, as well as the porous and reactive silica-containing RHA, which accelerates ion transport mobility and quickens the dissolution process of aluminosilicate precursors, resulting in polycondensation reactions and increased UCS of MSG grout [100]. The presence of RHA contributes to the filling of micropores through its filling effect and ascribes more amorphous gel phases, resulting in a dense and strengthened structure. Additionally, the RHA-active biogenic silica promotes the creation of additional calcium silicate hydrate phases in the calcium oxide-retaining geopolymer system, as RHA exhibits pozzolanic activity in the presence of Ca^{2+}ions [74]. A. Mehta, R. Siddique [101] observed that compressive strength increased by RHA with slag substitution up to 15 wt%. It is attributed to the higher SiO_2/Al_2O_3 ratio and increased the system's reactivity, resulting in secondary calcium silicate hydrate production with sodium alumina-sulfate hydrate. However, the presence of excessive RHA (>30 wt %) decreased the UCS by 13% compared to a 20% RHA presence. The higher content of RHA leads to a high percentage of unreacted or partially reacted RHA particles in the geopolymer matrix in the course of which weaker and less ductile geopolymer gel is produced [76]. The higher amount of SiO_2 delays the reaction of Si and Al ions and produces a lower density geopolymer binder resulting in lower compressive strength

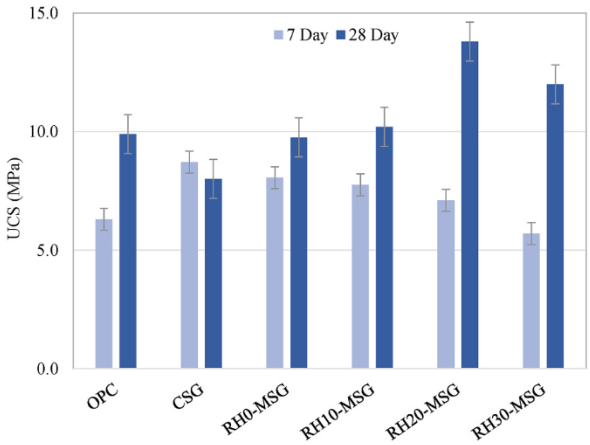

Fig. 8. UCS of OPC, CSG, and MSG grout.

[96]. Silva et al. [102] reported that the Si/Al ratio had a substantial impact on the mechanical features of the geopolymer. After this, using a high Si/Al ratio, low-crosslinked aluminosilicate materials with reduced strengths were developed. Furthermore, Kusbiantoro et al. [100] reported that the difference in the degree of solubility between slag and RHA reduces the rate of dissolution and poly-condensation of aluminosilicate compounds, hence the decrease in the strength at higher RHA content.

From the perspective of the activation method, the mechanochemical mechanism significantly impacted the strength performance of MSG grout specimens. The UCS values of CSG grout were lower than its counterpart MSG (Fig. 8); the UCS was reduced by 18% compared to RH0-MSG due to the higher cracks observed at 28 days, as shown in Fig. 9. Notably, the strength performance of the mixes containing 100% slag activated conventionally was reduced at a longer curing period. The UCS of the CSG grout sample was 8.7 MPa and 8 MPa at 7 days and 28 days, respectively. Moreover, the shape of the CSG grout sample at 28 days revealed apparent micro-cracks on the surface of the specimen, as seen in Fig. 8. These cracks can be attributed to the fact that there is more apparent shrinkage after 28 days compared to 7 days [37,103]. Additionally, mechanochemical activation presses increased the surface area and reaction rate of slag; as a result, an extra gel was generated as a consequence of the main reaction, which then accumulated and filled the pore system. The formation of a large proportion of gel in the geopolymer mixture improved the overall pore volume and porosity of the geopolymer grout, resulting in enhanced immobilization [37]. Similar MSG grout behavior was reported in Refs. [30,104,105]. On the other hand, the results revealed that the UCS of the OPC sample was a little higher than that of the RH0-MSG and CSG mixes due to the high shrinkage of slag and lower calcium content compared to OPC at 28 days. For example, the UCS of OPC is 1.4%, 19% higher than RH0-MSG and CSG, and 28% lower than RH20-MSG, respectively (Fig. 9). It can be concluded that the UCS of RH20-MSG $\geq$ OPC $\geq$ CSG grouts; therefore, the RHA can be effectively used in mechanochemical geopolymer grout up to 20% replacement.

3.4.2. *Ultrasonic pulse velocity and bulk density*

Fig. 10 presents the influence of RHA contents on ultrasonic pulse velocity (UPV) and bulk density tests of grouts. It can be seen from Fig. 10 that the UPV values of MSG grout were enhanced significantly at curing ages of 7 and 28 days. Based on the UPV classification presented in Table 3, all obtained specimens' hardened states ranged from low velocity to very low velocity [69]. It is obvious that specimens with varying levels of RHA incorporation enhance UPV after 28 days compared to 7 days (Fig. 10), owing to the combined strengthening effect of the bond reaction and the filling effect of the dissolved SiO_2 particles at later ages [94].

The UPV of MSG grout increased with increasing partial substitution of slag with RHA up to 20%, and declined thereafter (Fig. 10). The UPV of the MSG grout improved by 3% and 7% when RHA content increased from 10% to 20%. The improvement in UPV performance can be ascribed to introducing more silicon ions into the aluminosilicate network produced by RHA [106]. Istuque et al. [50] observed that the dissolution of RHA increased the strength and sustainability of alkali-activated mortars. Furthermore, an optimal balance between the filling effect and gel phase formation is achieved. It implies that the addition of RHA plays an important role in the refinement of pore structure. In the alkali activator environment, the silicon oxide particles were dissolved from the layered pore channels in RHA, resulting in additional silicon oxide micro-particles that acted as fillers for the whole pastes while participating in the reaction [73].

However, the UPV of RH30-MSG decreased by 1.5% when slag was replaced with 30% compared to the RH20-MSG mix. This decrease is probably attributable to changes in elemental composition [106]. Based on the chemical composition of raw materials (see Table 1), the inclusion of RHA into a slag-based mechanochemical geopolymer increases the SiO_2 content while decreasing the Al_2O_3 and CaO content in the reaction systems. Chemical component variations in the initial systems will affect the hydrated products and thus the material characteristics [107]. Meanwhile, excessive RHA creates a looser structure resulting from incomplete chemical reactions, as well as an increase in the number of unreacted components in the system. This unfilled honeycomb hole produces a non-homogeneous microstructure, which increases water absorption [48].

Additionally, the results reveal that the activation mechanism of geopolymer grout significantly affected the UPV values (Fig. 10). The UPV values of MSG samples were higher than those of CSG samples due to the fact that grinding the precursor increased the surface area and decreased the particle size of the slag and RHA particles, hence reducing the porosity and raising the density of the geopolymer grout. In addition, the grinding process considerably expedited the polymerization process by generating extra

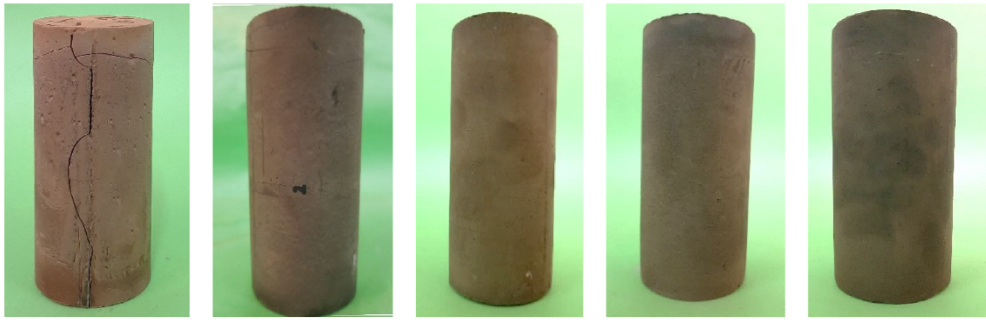

Fig. 9. The visual appearance of CSG and MSG grout.

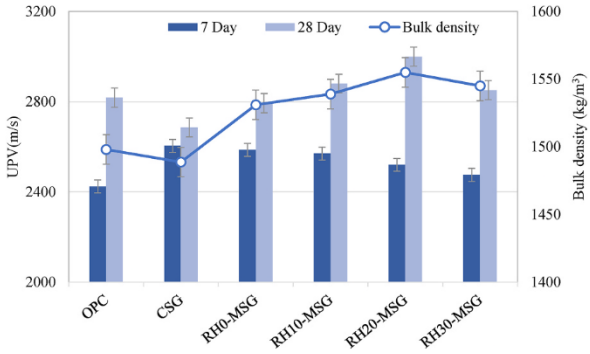

Fig. 10. UPV of OPC, CSG, and MSG grout.

aluminosilicate gel in the mixture, thereby increasing the density of MSG grout [35].

A bulk density test was conducted for grout to validate ultrasonic pulse velocity results, as displayed in Fig. 10. The bulk density follows a similar trend to the ultrasonic pulse velocity results regarding the RHA replacement. The highest bulk density of MSG grout was achieved at 20% RHA replacement among all MSG grouts after 28 days. In other words, the optimal replacement amount of slag by RHA was 20%, at which point the reaction extent of geopolymerization deepened, accompanied by a beneficial strength development and refinement of pore structure. However, it shows a slight decrease in bulk density values when the RHA addition dosage is increased to 30%. The decreased bulk density was primarily attributable to a reduced rate of aluminosilicate dissolution produced by the solubility difference between slag and RHA [100]. Furthermore, the higher concentration of unreactive silica due to increased slag replacement levels inhibited the polymerization process, resulting in reduced bulk density. As shown in Fig. 10, mechanochemical activation of slag-based geopolymer grout altered the bulk density values. The results demonstrated that MSG samples were denser than CSG and OPC samples since the density of RH0-MSG samples was 3% and 2% higher than that of CSG and OPC, respectively. The high density of MSG specimens resulted from the ball-milling of slag/RHA and chemical precursors, which raised the surface area and reactivity of the geopolymeric precursors. The higher reactivity of the source materials resulted in the development of more gel as the principal reaction product, decreasing the porosity and increasing the density of MSG grout [108].

3.5. *Microstructural analysis*

XRD patterns were utilized to analyze the influence of the activation mechanism of geopolymer grout, as depicted in Fig. 11. The XRD patterns of hardened CSG and RH0-MSG reveal the existence of the geopolymeric phases sodium aluminum silicate hydrate and sodium silicate hydrate in addition to the crystalline phase peaks observed in the raw powder [29]. These phases were much more intense in RH0-MSG than in CSG as a result of the mechanochemical grinding of slag and chemical powder. The (halo) amorphous phase and some sharp peaks of crystalline phases in the XRD traces indicated that both CSG and RH0-MSG were semi-crystalline with a substantial quantity of amorphous gel. This amorphous shape illustrates that the geopolymer contains a highly disordered glassy silicoaluminous phase.

Fig. 12 shows the effect activation method on the microstructure characterization of MSG and CSG grouts. Notably, the activation method had a considerable effect on the microstructure of geopolymer grout. As seen in Fig. 12a and b, many unreactive slag particles can be observed in CSG grout as compared to its counterpart RH0-MSG, which includes limited unreactive slag particles due to the beneficial effect of mechanochemically activated mechanism that increased surface area and reduced the particle size of slag, resulting in lower porosity and higher density in comparison with CSG grout. Additionally, significant cracks can be seen in CSG grout (Fig. 12a) because of the poor connectivity of the reaction products [37]. It can be concluded that the mechanochemically activated method is

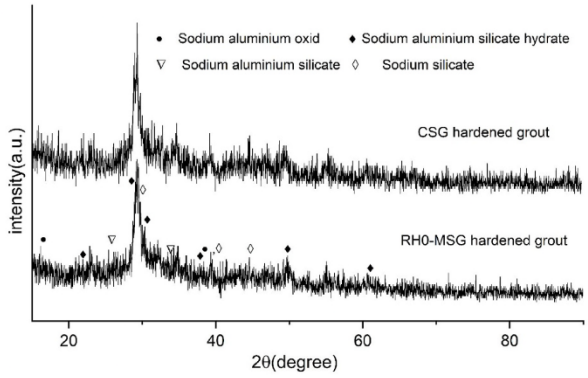

Fig. 11. XRD patterns of CSG and RH0-MSG hardened grout.

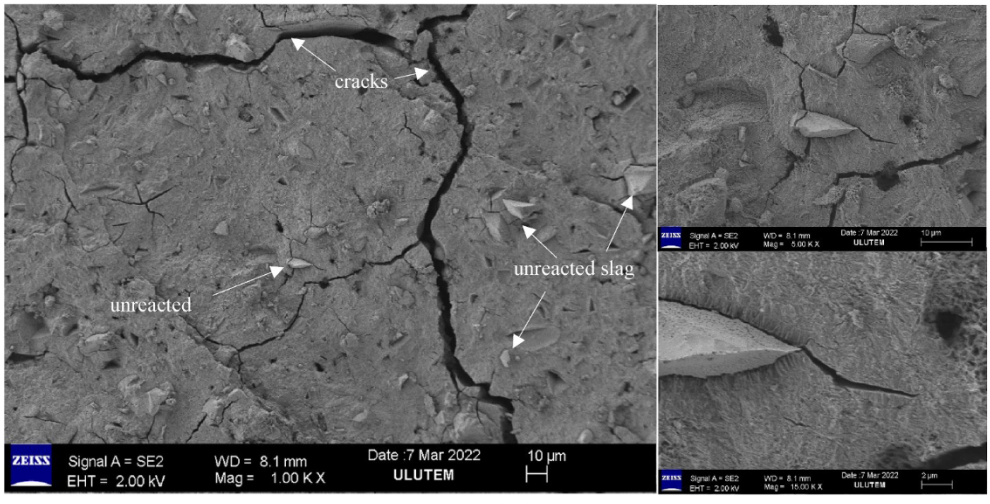

(a)

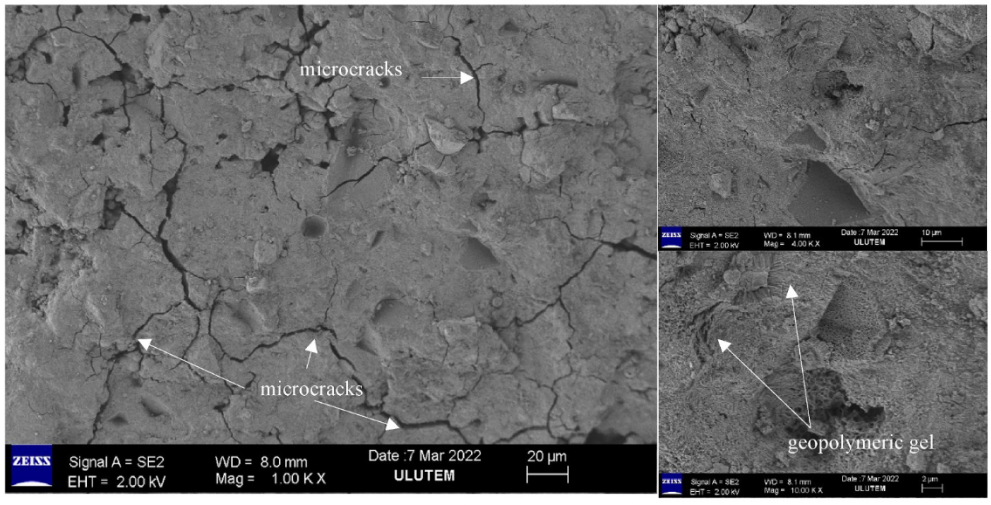

(b)

Fig. 12. SEM images of the hardened (a) CSG and (b) RH0-MSG grout.

more beneficial than the conventionally activated method in densifying the compactness of grout's microstructure, and thus, the mechanical properties of MSG grout have been greatly enhanced. Furthermore, the geopolymerization reaction of MSG grout was dramatically enhanced during the grinding process due to the creation of additional aluminosilicate gel in the mix (Fig. 12b); the produced gel has a more homogeneous microstructure which decreased the porosity and enhanced the reaction rate of slag particles.

Fig. 13 presents the influence of RHA amount on the microstructure characterization of MSG grout. As seen in Fig. 13b, a 20% RHA replacement results in a compact structure and acts more homogeneously with formed gels and less unreacted particles than the microstructures of RH0- MSG (Fig. 12b) and RH30- MSG (Fig. 13b). In other words, the microstructure of the RH20- MSG is denser with less pores or visible cracks. The incorporation of 20% RHA contributes to the filling effect or interpenetrating action between the presence of other components in the geopolymer, leading to a decrease in average pore diameters and a more compact structure [48, 75]. This decreases the geopolymer's permeation properties, such as its external ion penetration rate (such as chloride ion permeability) and low sorptivity [48]. As a result, a 20% replacement of slag by RHA improved the mechanical performance of MSG grout, and this observation aligns well with previous studies [94,101,109].

At 30% RHA, the microstructure of the RH30-MSG is still denser and more compact than RH0-MSG; however, it continued to allow a significant number of unreacted RHA particles with many microcracks (Fig. 13b). These microcracks could have been caused by an excess of RHA, which inhibits the synthesis of reaction products with crosslinking structures.

Due to the excessive amount of RHA, the interface between the RHA particles and the MSG matrix was reduced. Therefore, the low mechanical interlocking and the formed microcracks resulted in lower densification and lower mechanical performance of RH30-MSG samples compared to RH20-MSG samples, as shown in Fig. 13b [110]. This effect is due to the considerable decrease in alumina with

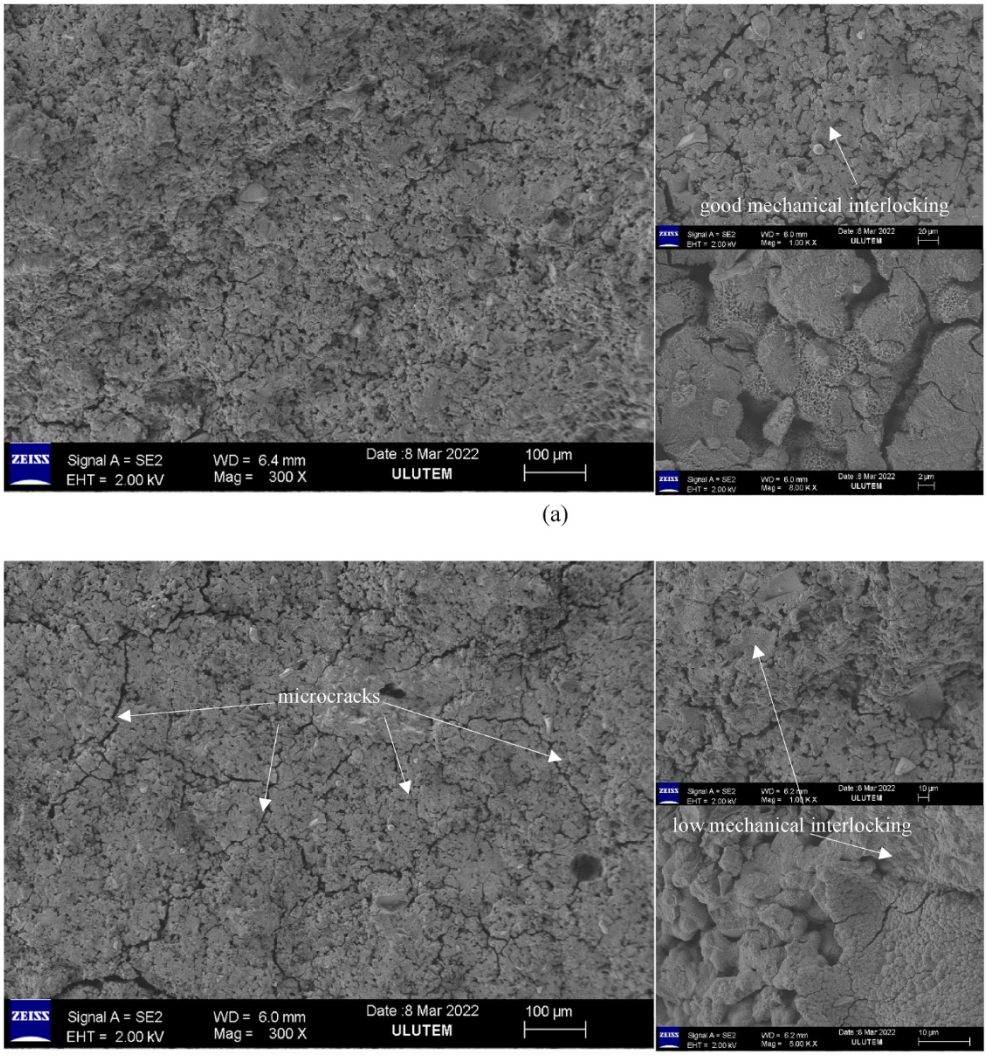

Fig. 13. SEM images of the hardened (a) RH20- MSG and (b) RH30- MSG grout.

increasing RHA content, since alumina content is important in the production of a stable polymer network [111]. Meanwhile, the elevated level of RHA brings about a looser structure caused by inadequate chemical reactions and increased unreacted components in the system [48]. As a result, partial slag replacement by 30% RHA reduces the UCS of the mechanochemical activation geopolymer grout.

4. Conclusions

This research aimed to develop mechanochemically activated geopolymeric grout with an environmentally and more user-friendly approach. Current geopolymer synthesis methods address the limitations of conventional geopolymerization techniques. In addition, the feasibility of incorporating RHA as a partial precursor in slag-based mechanochemically activated geopolymer grout was investigated. Pointedly, a conventionally activated geopolymer-based grout and an ordinary Portland cement grout were investigated for comparison. All studied groups were examined for their rheological, fresh, mechanical, and microstructural performances. The following conclusions are derived from the results of the study:

- The presence of RHA as a partial substitution for slag in MSG grout has a noticeable effect with a beneficial consequence on the improvement of the rheological responses of the grout as evidenced by the decrease in apparent viscosity and shear stress of RHA-containing mixes. In addition, the mechanochemical activation approach positively affected the rheological properties of geopolymer grout.

- The yield stress and plastic viscosity values of the MSG grout were reduced by 5–38% and 9–41% when slag was substituted with 0–30% RHA, respectively. Regarding the effect of the activation mechanism, the MSG grout exhibited between a 4% and 27% lower yield stress and plastic viscosity than the CSG grout. In addition, the results indicated that the yield stress and plastic viscosity of OPC grout were higher than those of MSG and CSG grout.
- The activation method and RHA replacement substantially impacted the setting time. Utilizing 0–30% RHA prolonged the initial and final setting times of MSG grout by 14–44% and 6–42%, respectively. In contrast, mechanochemical activation significantly accelerated the setting process. Initial setting times for MSG, CSG, and OPC were 3.3 h, and 8 h, respectively, whereas final setting times were 4.5 h, 6.3 h, and 12 h, respectively.
- The bleeding capacity of MSG grout increased from 0.025% to 0.1% as RHA content increased from 0 to 30% due to its low water demand and filling impact compared to slag. In addition, the results demonstrated that the MSG grout had a substantially lower capacity for bleeding than the CSG and OPC grout. It was found that as a result of the reduction in particle size and the rise in the powder's surface area caused by the grinding process, a greater quantity of water is required to adequately cover the surface of the particles.
- The substitution of 10–20% slag with rice husk ash enhanced the UCS of MSG grouts by 4.5–41% due to the introduction of more active silicon into the geopolymerization reaction process by rice husk ash, hence promoting the formation of additional gel phases. In addition, the mechanochemical technique increased the strength of geopolymer grout by 18% compared to its conventional counterpart.
- The microstructure analysis confirmed that the activation method significantly impacted the microstructure of geopolymer grout because the grinding process increased slag surface area while decreasing particle size, resulting in geopolymer grout samples with lower porosity and higher density than conventionally activated samples. Inclusive of this, the SEM images revealed that the microstructure of MSG grout at 20% RHA was densely compacted with fewer pores or no apparent cracks as a result of the incorporation of more active silicon into the geopolymerization reaction process, which promoted the generation of additional gel phases, which was also the strong support for the UCS development of MSG grout.

Author statement

Israa Sabbar Abbas: Conceptualization, Writing- Original draft preparation, Methodology, Software, Investigation.
Mukhtar Hamid Abed: Data curation, Investigation, Validation, Writing- Reviewing and Editing.
Hanifi Canakci: Supervision, Reviewing and Editing.

Declaration of competing interest

The authors declare that they have no known competing financial interests or personal relationships that could have appeared to influence the work reported in this paper.

Data availability

No data was used for the research described in the article.

References

[1] M. Chang, T. Mao, R. Huang, A study on the improvements of geotechnical properties of in-situ soils by grouting, Geomech. \& Eng. 10 (2016) 527–546.
[2] E.N. Bellendir, A.V. Aleksandrov, M.G. Zertsalov, A.N. Simutin, Building and structure protection and leveling using compensation grouting technology, Power Technol. Eng. 50 (2016) 142–146, https://doi.org/10.1007/s10749-016-0674-y.
[3] J. Qiu, H. Liu, J. Lai, H. Lai, J. Chen, K. Wang, Investigating the long-term settlement of a tunnel built over improved loessial foundation soil using jet grouting technique, J. Perform. Constr. Facil. 32 (2018), https://doi.org/10.1061/(asce)cf.1943-5509.0001155.
[4] X. Wang, J. Lai, R.S. Garnes, Y. Luo, Support system for tunnelling in squeezing ground of qingling-daba mountainous area: a case study from soft rock tunnels, Adv. Civ. Eng. 2019 (2019), https://doi.org/10.1155/2019/8682535.
[5] Z. Li, H. You, Y. Gao, C. Wang, J. Zhang, Effect of ultrafine red mud on the workability and microstructure of blast furnace slag-red mud based geopolymeric grouts, Powder Technol 392 (2021) 610–618, https://doi.org/10.1016/j.powtec.2021.07.046.
[6] M. Schneider, M. Romer, M. Tschudin, H. Bolio, Sustainable cement production-present and future, Cem. Concr. Res. 41 (2011) 642–650, https://doi.org/10.1016/j.cemconres.2011.03.019.
[7] Q. Liu, X. Li, M. Cui, J. Wang, X. Lyu, Preparation of eco-friendly one-part geopolymers from gold mine tailings by alkaline hydrothermal activation, J. Clean. Prod. 298 (2021), 126806, https://doi.org/10.1016/j.jclepro.2021.126806.
[8] E. Gartner, Industrially interesting approaches to "low-CO2" cements, Cem. Concr. Res. 34 (2004) 1489–1498, https://doi.org/10.1016/j.cemconres.2004.01.021.
[9] X.S. Shi, F.G. Collins, X.L. Zhao, Q.Y. Wang, Mechanical properties and microstructure analysis of fly ash geopolymeric recycled concrete, J. Hazard. Mater. 237–238 (2012) 20–29, https://doi.org/10.1016/j.jhazmat.2012.07.070.
[10] L.K. Turner, F.G. Collins, Carbon dioxide equivalent (CO2-e) emissions: a comparison between geopolymer and OPC cement concrete, Constr. Build. Mater. 43 (2013) 125–130, https://doi.org/10.1016/j.conbuildmat.2013.01.023.
[11] J. Xie, O. Kayali, Effect of initial water content and curing moisture conditions on the development of fly ash-based geopolymers in heat and ambient temperature, Constr. Build. Mater. 67 (2014) 20–28, https://doi.org/10.1016/j.conbuildmat.2013.10.047.
[12] G. Humur, A. Çevik, Effects of hybrid fibers and nanosilica on mechanical and durability properties of lightweight engineered geopolymer composites subjected to cyclic loading and heating–cooling cycles, Constr. Build. Mater. 326 (2022), 126846, https://doi.org/10.1016/j.conbuildmat.2022.126846.
[13] M. Palacios, P.F.G. Banfill, F. Puertas, Rheology and setting of alkali-activated slag pastes and mortars: effect of organic admixture, ACI Mater. J. 105 (2008) 140.
[14] S. Aydın, B. Baradan, Sulfate resistance of alkali-activated slag and Portland cement based reactive powder concrete, J. Build. Eng. 43 (2021), 103205, https://doi.org/10.1016/j.jobe.2021.103205.

[15] J. Zhang, S. Li, Z. Li, Q. Zhang, H. Li, J. Du, Y. Qi, Properties of fresh and hardened geopolymer-based grouts, Ceram. - Silikaty. 63 (2019) 164–173, https://doi.org/10.13168/cs.2019.0008.

[16] M. Komljenović, Z. Baščarević, N. Marjanović, V. Nikolić, External sulfate attack on alkali-activated slag, Constr. Build. Mater. 49 (2013) 31–39, https://doi.org/10.1016/j.conbuildmat.2013.08.013.

[17] S. Siddique, V. Gupta, S. Chaudhary, S. Park, J.G. Jang, Influence of the precursor, molarity and temperature on the rheology and structural buildup of alkali-activated materials, Materials (Basel) 14 (2021), https://doi.org/10.3390/ma14133590.

[18] N. Ye, J. Yang, S. Liang, Y. Hu, J. Hu, B. Xiao, Q. Huang, Synthesis and strength optimization of one-part geopolymer based on red mud, Constr. Build. Mater. 111 (2016) 317–325.

[19] P. Duxson, J.L. Provis, Designing precursors for geopolymer cements, J. Am. Ceram. Soc. 91 (2008) 3864–3869, https://doi.org/10.1111/j.1551-2916.2008.02787.x.

[20] P. Sturm, G.J.G. Gluth, H.J.H. Brouwers, H.-C. Kühne, Synthesizing one-part geopolymers from rice husk ash, Constr. Build. Mater. 124 (2016) 961–966.

[21] L. Coppola, D. Co, E. Crotti, G. Gazzaniga, T. Pastore, The Durability of One-Part Alkali-Activated Slag-Based Mortars in Di Ff Erent Environments, 2020.

[22] L. Li, J.X. Lu, B. Zhang, C.S. Poon, Rheology behavior of one-part alkali activated slag/glass powder (AASG) pastes, Constr. Build. Mater. 258 (2020), 120381, https://doi.org/10.1016/j.conbuildmat.2020.120381.

[23] M. Hamid Abed, I.S. Abbas, H. Canakci, Influence of mechanochemical activation on the rheological, fresh, and mechanical properties of one-part geopolymer grout, Adv. Cem. Res. (2022) 1–38.

[24] D. Koloušek, J. Brus, M. Urbanova, J. Andertova, V. Hulinsky, J. Vorel, Preparation, structure and hydrothermal stability of alternative (sodium silicate-free) geopolymers, J. Mater. Sci. 42 (2007) 9267–9275.

[25] A. Hajimohammadi, J.L. Provis, J.S.J. Van Deventer, One-part geopolymer mixes from geothermal silica and sodium aluminate, Ind. Eng. Chem. Res. 47 (2008) 9396–9405.

[26] P. Sturm, G.J.G. Gluth, S. Simon, H.J.H. Brouwers, H.C. Kühne, The effect of heat treatment on the mechanical and structural properties of one-part geopolymer-zeolite composites, Thermochim. Acta. 635 (2016) 41–58, https://doi.org/10.1016/j.tca.2016.04.015.

[27] J. Ren, H. Sun, Q. Li, Z. Li, L. Ling, X. Zhang, Y. Wang, F. Xing, Experimental comparisons between one-part and normal (two-part) alkali-activated slag binders, Constr. Build. Mater. 309 (2021), 125177, https://doi.org/10.1016/j.conbuildmat.2021.125177.

[28] G. Masi, A. Filipponi, M.C. Bignozzi, Fly ash-based one-part alkali activated mortars cured at room temperature: effect of precursor pre-treatments, Open Ceram 8 (2021), 100178, https://doi.org/10.1016/j.oceram.2021.100178.

[29] R. Gupta, P. Bhardwaj, D. Mishra, M. Mudgal, R.K. Chouhan, M. Prasad, S.S. Amritphale, Evolution of advanced geopolymeric cementitious material via a novel process, Adv. Cem. Res. 29 (2017) 125–134, https://doi.org/10.1680/jadcr.16.00113.

[30] S. Hosseini, N.A. Brake, M. Nikookar, Ö. Günaydın-Şen, H.A. Snyder, Mechanochemically activated bottom ash-fly ash geopolymer, Cem. Concr. Compos. 118 (2021), https://doi.org/10.1016/j.cemconcomp.2021.103976.

[31] G. Intini, L. Liberti, M. Notarnicola, F. Di Canio, Mechanochemical Activation of Coal Fly Ash for Production of High Strength Cement Conglomerates, vol. 17, 2009, pp. 567–571. ХиМия в Интересах Устойчивого Развития.

[32] P. Baláž, M. Achimovičová, M. Baláž, P. Billik, Z. Cherkezova-Zheleva, J.M. Criado, F. Delogu, E. Dutková, E. Gaffet, F.J. Gotor, others, Hallmarks of mechanochemistry: from nanoparticles to technology, Chem. Soc. Rev. 42 (2013) 7571–7637.

[33] A. Souri, H. Kazemi-Kamyab, R. Snellings, R. Naghizadeh, F. Golestani-Fard, K. Scrivener, Pozzolanic activity of mechanochemically and thermally activated kaolins in cement, Cem. Concr. Res. 77 (2015) 47–59.

[34] J. Temuujin, R.P. Williams, A. Van Riessen, Effect of mechanical activation of fly ash on the properties of geopolymer cured at ambient temperature, J. Mater. Process. Technol. 209 (2009) 5276–5280.

[35] S. Kumar, R. Kumar, Mechanical activation of fly ash: effect on reaction, structure and properties of resulting geopolymer, Ceram. Int. 37 (2011) 533–541.

[36] S. Kushwah, M. Mudgal, R.K. Chouhan, The Process, Characterization and Mechanical properties of fly ash-based Solid form geopolymer via mechanical activation, South African J. Chem. Eng. 38 (2021) 104–114, https://doi.org/10.1016/j.sajce.2021.09.002.

[37] M. Hamid Abed, I. Sabbar Abbas, M. Hamed, H. Canakci, Rheological, fresh, and mechanical properties of mechanochemically activated geopolymer grout: a comparative study with conventionally activated geopolymer grout, Constr. Build. Mater. 322 (2022), 126338, https://doi.org/10.1016/j.conbuildmat.2022.126338.

[38] Y. Wang, X. Wang, Y. Lou, F. Gao, W. Wu, Effect of mechanical activation on reaction mechanism of one-part preparation fly ash/slag-based geopolymer, Adv. Cem. Res. (2022) 1–15.

[39] H. Kizhakkumodom Venkatanarayanan, P.R. Rangaraju, Effect of grinding of low-carbon rice husk ash on the microstructure and performance properties of blended cement concrete, Cem. Concr. Compos. 55 (2015) 348–363, https://doi.org/10.1016/j.cemconcomp.2014.09.021.

[40] P.K. Mehta, Properties of blended cements made from rice husk ash, J. Proc. (1977) 440–442.

[41] N.M. Azad, S.M.S.M.K. Samarakoon, Utilization of industrial by-products/waste to manufacture geopolymer cement/concrete, Sustain 13 (2021) 1–22, https://doi.org/10.3390/su13020873.

[42] N. Wen, Y. Zhao, Z. Yu, M. Liu, A sludge and modified rice husk ash-based geopolymer: synthesis and characterization analysis, J. Clean. Prod. 226 (2019) 805–814.

[43] Y. Li, X. Ding, Y. Guo, C. Rong, L. Wang, Y. Qu, X. Ma, Z. Wang, A new method of comprehensive utilization of rice husk, J. Hazard. Mater. 186 (2011) 2151–2156, https://doi.org/10.1016/j.jhazmat.2011.01.013.

[44] H.B. Mahmud, E. Majuar, M.F.M. Zain, N. Hamid, Mechanical properties and durability of high strength concrete containing rice husk ash, Spec. Publ. 221 (2004) 751–766.

[45] J.M. Mejía, R. Mejía de Gutiérrez, F. Puertas, Ceniza de cascarilla de arroz como fuente de sílice en sistemas cementicios de ceniza volante y escoria activados alcalinamente, Mater. Constr. 63 (2013) 361–375, https://doi.org/10.3989/mc.2013.04712.

[46] T. Luukkonen, Z. Abdollahnejad, J. Yliniemi, P. Kinnunen, M. Illikainen, Comparison of alkali and silica sources in one-part alkali-activated blast furnace slag mortar, J. Clean. Prod. 187 (2018) 171–179, https://doi.org/10.1016/j.jclepro.2018.03.202.

[47] G. Liang, H. Zhu, Z. Zhang, Q. Wu, Effect of rice husk ash addition on the compressive strength and thermal stability of metakaolin based geopolymer, Constr. Build. Mater. 222 (2019) 872–881, https://doi.org/10.1016/j.conbuildmat.2019.06.200.

[48] H. Zhu, G. Liang, J. Xu, Q. Wu, M. Zhai, Influence of rice husk ash on the waterproof properties of ultrafine fly ash based geopolymer, Constr. Build. Mater. 208 (2019) 394–401, https://doi.org/10.1016/j.conbuildmat.2019.03.035.

[49] F. Celik, H. Canakci, An investigation of rheological properties of cement-based grout mixed with rice husk ash (RHA), Constr. Build. Mater. 91 (2015) 187–194.

[50] D.B. Istuque, J. Payá, L. Soriano, M.V. Borrachero, J. Monzó, M.M. Tashima, The role of dissolved rice husk ash in the development of binary blast furnace slag-sewage sludge ash alkali-activated mortars, J. Build. Eng. 52 (2022), https://doi.org/10.1016/j.jobe.2022.104472.

[51] F. Matalkah, L. Xu, W. Wu, P. Soroushian, Mechanochemical synthesis of one-part alkali aluminosilicate hydraulic cement, Mater. Struct. 50 (2017) 1–12.

[52] C. Fluids, Standard test method for viscosity of chemical grouts by brookfield viscometer, Annu. B. ASTM Stand. (2003) 8–10, https://doi.org/10.1520/D4016-08.2, 04.

[53] H. Güllü, A. Ali Agha, The rheological, fresh and strength effects of cold-bonded geopolymer made with metakaolin and slag for grouting, Constr. Build. Mater. 274 (2021), 122091, https://doi.org/10.1016/j.conbuildmat.2020.122091.

[54] H. Güllü, A. Cevik, K.M.A. Al-Ezzi, M.E. Gülsan, On the rheology of using geopolymer for grouting: a comparative study with cement-based grout included fly ash and cold bonded fly ash, Constr. Build. Mater. 196 (2019) 594–610.

[55] H. Güllü, M.M.D. Al Nuaimi, A. Aytek, Rheological and strength performances of cold-bonded geopolymer made from limestone dust and bottom ash for grouting and deep mixing, Bull. Eng. Geol. Environ. 80 (2021) 1103–1123, https://doi.org/10.1007/s10064-020-01998-2.

[56] M. Şahmaran, The effect of replacement rate and fineness of natural zeolite on the rheological properties of cement-based grouts, Can. J. Civ. Eng. 35 (2008) 796–806.
[57] A. Yahia, K.H. Khayat, Analytical models for estimating yield stress of high-performance pseudoplastic grout, Cem. Concr. Res. 31 (2001) 731–738.
[58] C.K. Park, M.H. Noh, T.H. Park, Rheological properties of cementitious materials containing mineral admixtures, Cem. Concr. Res. 35 (2005) 842–849.
[59] B. Widjaja, S.H.-H. Lee, Flow box test for viscosity of soil in plastic and viscous liquid states, Soils Found 53 (2013) 35–46.
[60] A. Yahia, S. Mantellato, R.J. Flatt, Concrete rheology: a basis for understanding chemical admixtures, in: Sci. Technol. Concr. Admixtures, Elsevier, 2016, pp. 97–127.
[61] H. Güllü, Comparison of rheological models for jet grout cement mixtures with various stabilizers, Constr. Build. Mater. 127 (2016) 220–236, https://doi.org/10.1016/j.conbuildmat.2016.09.129.
[62] D. Feys, J.E. Wallevik, A. Yahia, K.H. Khayat, O.H. Wallevik, Extension of the Reiner-Riwlin equation to determine modified Bingham parameters measured in coaxial cylinders rheometers, Mater. Struct. Constr. 46 (2013) 289–311, https://doi.org/10.1617/s11527-012-9902-6.
[63] Y. Rifaai, A. Yahia, A. Mostafa, S. Aggoun, E.H. Kadri, Rheology of fly ash-based geopolymer: effect of NaOH concentration, Constr. Build. Mater. 223 (2019) 583–594, https://doi.org/10.1016/j.conbuildmat.2019.07.028.
[64] American Society for Testing & Mater, Standard Test Methods for Felt, 1987, pp. 1–8, https://doi.org/10.1520/C0191-19.2.
[65] ASTM:C940-10a, Standard Test Method for Expansion and Bleeding of Freshly Mixed Grouts for Preplaced-Aggregate Concrete in the Laboratory, ASTM Int. i, 2010, pp. 1–3, https://doi.org/10.1520/C0940-16.2.
[66] C.C. Test, C. Ag, A. Concrete, P. Concrete, StandardTest Method for Compressive Strength of Grouts for Preplaced-Aggregate Concrete in the Laboratory, vol. 1, 2021, pp. 10–12.
[67] D. Dimensional, S. Tolerances, Standard Test Method for Unconfined Compressive Strength of Intact Rock Core, 2021, pp. 14–16, 03.
[68] C. Astm, Standard Test Method for Pulse Velocity through Concrete, ASTM Int. West, Conshohocken, PA, 2009.
[69] O.H. Anon, Classification of rocks and soils for engineering geological mapping. Part 1: rock and soil materials, Bull Int Assoc Eng Geol 19 (1979) 355–371.
[70] J. Baalamurugan, V. Ganesh Kumar, T. Stalin Dhas, S. Taran, S. Nalini, V. Karthick, M. Ravi, K. Govindaraju, Utilization of induction furnace steel slag based iron oxide nanocomposites for antibacterial studies, SN Appl. Sci. 3 (2021) 1–8, https://doi.org/10.1007/s42452-021-04299-9.
[71] Y.J. Zhang, Y.L. Zhao, H.H. Li, D.L. Xu, Structure characterization of hydration products generated by alkaline activation of granulated blast furnace slag, J. Mater. Sci. 43 (2008) 7141–7147, https://doi.org/10.1007/s10853-008-3028-9.
[72] M.O. Yusuf, M.A.M. Johari, Z.A. Ahmad, M. Maslehuddin, Effects of addition of Al(OH)3 on the strength of alkaline activated ground blast furnace slag-ultrafine palm oil fuel ash (AAGU) based binder, Constr. Build. Mater. 50 (2014) 361–367, https://doi.org/10.1016/j.conbuildmat.2013.09.054.
[73] H. Zhu, G. Liang, Z. Zhang, Q. Wu, J. Du, Partial replacement of metakaolin with thermally treated rice husk ash in metakaolin-based geopolymer, Constr. Build. Mater. 221 (2019) 527–538, https://doi.org/10.1016/j.conbuildmat.2019.06.112.
[74] S.S. Hossain, P.K. Roy, C.J. Bae, Utilization of waste rice husk ash for sustainable geopolymer: a review, Constr. Build. Mater. 310 (2021), 125218, https://doi.org/10.1016/j.conbuildmat.2021.125218.
[75] S. Dadsetan, H. Siad, M. Lachemi, M. Sahmaran, Extensive evaluation on the effect of glass powder on the rheology, strength, and microstructure of metakaolin-based geopolymer binders, Constr. Build. Mater. 268 (2021), 121168, https://doi.org/10.1016/j.conbuildmat.2020.121168.
[76] Y.J. Patel, N. Shah, Enhancement of the properties of ground granulated blast furnace slag based self compacting geopolymer concrete by incorporating rice husk ash, Constr. Build. Mater. 171 (2018) 654–662.
[77] R.K. Chouhan, M. Mudgal, A. Bisarya, A.K. Srivastava, Rice-husk-based superplasticizer to increase performance of fly ash geopolymer concrete, Emerg. Mater. Res. 7 (2018) 169–177, https://doi.org/10.1680/jemmr.18.00035.
[78] D.W. Zhang, D. min Wang, Z. Liu, F. zhu Xie, Rheology, agglomerate structure, and particle shape of fresh geopolymer pastes with different NaOH activators content, Constr. Build. Mater. 187 (2018) 674–680, https://doi.org/10.1016/j.conbuildmat.2018.07.205.
[79] N. Marjanović, M. Komljenović, Z. Baščarević, V. Nikolić, Improving reactivity of fly ash and properties of ensuing geopolymers through mechanical activation, Constr. Build. Mater. 57 (2014) 151–162, https://doi.org/10.1016/j.conbuildmat.2014.01.095.
[80] T. Yang, H. Zhu, Z. Zhang, X. Gao, C. Zhang, Q. Wu, Effect of fly ash microsphere on the rheology and microstructure of alkali-activated fly ash/slag pastes, Cem. Concr. Res. 109 (2018) 198–207, https://doi.org/10.1016/j.cemconres.2018.04.008.
[81] D.P. Bentz, C.F. Ferraris, M.A. Galler, A.S. Hansen, J.M. Guynn, Influence of particle size distributions on yield stress and viscosity of cement-fly ash pastes, Cem. Concr. Res. 42 (2012) 404–409, https://doi.org/10.1016/j.cemconres.2011.11.006.
[82] S. Kumar, R. Kumar, S.P. Mehrotra, Influence of granulated blast furnace slag on the reaction, structure and properties of fly ash based geopolymer, J. Mater. Sci. 45 (2010) 607–615, https://doi.org/10.1007/s10853-009-3934-5.
[83] S. Samantasinghar, S.P. Singh, Fresh and hardened properties of fly ash–slag blended geopolymer paste and mortar, Int. J. Concr. Struct. Mater. 13 (2019) 1–12, https://doi.org/10.1186/s40069-019-0360-1.
[84] P. Nath, P.K. Sarker, Effect of GGBFS on setting, workability and early strength properties of fly ash geopolymer concrete cured in ambient condition, Constr. Build. Mater. 66 (2014) 163–171.
[85] Y. Zhang, X. Luo, X. Kong, F. Wang, L. Gao, Rheological properties and microstructure of fresh cement pastes with varied dispersion media and superplasticizers, Powder Technol 330 (2018) 219–227, https://doi.org/10.1016/j.powtec.2018.02.014.
[86] A. Zingg, F. Winnefeld, L. Holzer, J. Pakusch, S. Becker, L. Gauckler, Adsorption of polyelectrolytes and its influence on the rheology, zeta potential, and microstructure of various cement and hydrate phases, J. Colloid Interface Sci. 323 (2008) 301–312.
[87] G. Liang, H. Li, H. Zhu, T. Liu, Q. Chen, H. Guo, Reuse of waste glass powder in alkali-activated metakaolin/fly ash pastes: physical properties, reaction kinetics and microstructure, Resour. Conserv. Recycl. 173 (2021), 105721, https://doi.org/10.1016/j.resconrec.2021.105721.
[88] A. Kashani, J.L. Provis, G.G. Qiao, J.S.J. Van Deventer, The interrelationship between surface chemistry and rheology in alkali activated slag paste, Constr. Build. Mater. 65 (2014) 583–591, https://doi.org/10.1016/j.conbuildmat.2014.04.127.
[89] B.J. Konijn, O.B.J. Sanderink, N.P. Kruyt, Experimental study of the viscosity of suspensions: effect of solid fraction, particle size and suspending liquid, Powder Technol 266 (2014) 61–69, https://doi.org/10.1016/j.powtec.2014.05.044.
[90] P. Chindaprasirt, P. De Silva, K. Sagoe-Crentsil, S. Hanjitsuwan, Effect of SiO 2 and Al 2O 3on the setting and hardening of high calcium fly ash-based geopolymer systems, J. Mater. Sci. 47 (2012) 4876–4883, https://doi.org/10.1007/s10853-012-6353-y.
[91] N. Billong, J. Kinuthia, J. Oti, U.C. Melo, Performance of sodium silicate free geopolymers from metakaolin (MK) and Rice Husk Ash (RHA): effect on tensile strength and microstructure, Constr. Build. Mater. 189 (2018) 307–313, https://doi.org/10.1016/j.conbuildmat.2018.09.001.
[92] G. Liang, H. Zhu, H. Li, T. Liu, H. Guo, Comparative study on the effects of rice husk ash and silica fume on the freezing resistance of metakaolin-based geopolymer, Constr. Build. Mater. 293 (2021), 123486, https://doi.org/10.1016/j.conbuildmat.2021.123486.
[93] H. Li, D. Xu, S. Feng, B. Shang, Microstructure and performance of fly ash micro-beads in cementitious material system, Constr. Build. Mater. 52 (2014) 422–427, https://doi.org/10.1016/j.conbuildmat.2013.11.040.
[94] G. Liang, H. Zhu, Z. Zhang, Q. Wu, J. Du, Investigation of the waterproof property of alkali-activated metakaolin geopolymer added with rice husk ash, J. Clean. Prod. 230 (2019) 603–612, https://doi.org/10.1016/j.jclepro.2019.05.111.
[95] H. Zhu, G. Liang, H. Li, Q. Wu, C. Zhang, Z. Yin, S. Hua, Insights to the sulfate resistance and microstructures of alkali-activated metakaolin/slag pastes, Appl. Clay Sci. 202 (2021), 105968, https://doi.org/10.1016/j.clay.2020.105968.
[96] T. Tho-In, V. Sata, K. Boonserm, P. Chindaprasirt, Compressive strength and microstructure analysis of geopolymer paste using waste glass powder and fly ash, J. Clean. Prod. 172 (2016) 2892–2898, https://doi.org/10.1016/j.jclepro.2017.11.125.
[97] V.S. Athira, A. Bahurudeen, M. Saljas, K. Jayachandran, Influence of different curing methods on mechanical and durability properties of alkali activated binders, Constr. Build. Mater. 299 (2021), https://doi.org/10.1016/j.conbuildmat.2021.123963.
[98] M.N.N. Khan, J.C. Kuri, P.K. Sarker, Effect of waste glass powder as a partial precursor in ambient cured alkali activated fly ash and fly ash-GGBFS mortars, J. Build. Eng. 34 (2021), 101934, https://doi.org/10.1016/j.jobe.2020.101934.

[99] A. Fernández-Jiménez, N. Cristelo, T. Miranda, Á. Palomo, Sustainable alkali activated materials: precursor and activator derived from industrial wastes, J. Clean. Prod. 162 (2017) 1200–1209, https://doi.org/10.1016/j.jclepro.2017.06.151.
[100] A. Kusbiantoro, M.F. Nuruddin, N. Shafiq, S.A. Qazi, The effect of microwave incinerated rice husk ash on the compressive and bond strength of fly ash based geopolymer concrete, Constr. Build. Mater. 36 (2012) 695–703, https://doi.org/10.1016/j.conbuildmat.2012.06.064.
[101] A. Mehta, R. Siddique, Sustainable geopolymer concrete using ground granulated blast furnace slag and rice husk ash: strength and permeability properties, J. Clean. Prod. 205 (2018) 49–57, https://doi.org/10.1016/j.jclepro.2018.08.313.
[102] P. De Silva, K. Sagoe-Crenstil, V. Sirivivatnanon, Kinetics of geopolymerization: role of Al2O3 and SiO2, Cem. Concr. Res. 37 (2007) 512–518, https://doi.org/10.1016/j.cemconres.2007.01.003.
[103] N.K. Lee, H.K. Lee, Setting and mechanical properties of alkali-activated fly ash/slag concrete manufactured at room temperature, Constr. Build. Mater. 47 (2013) 1201–1209, https://doi.org/10.1016/j.conbuildmat.2013.05.107.
[104] A. Fernández-Jiménez, I. Garcia-Lodeiro, O. Maltseva, A. Palomo, Mechanical-chemical activation of coal fly ashes: an effective way for recycling and make cementitious materials, Front. Mater. 6 (2019) 51.
[105] E. Adesanya, K. Ohenoja, J. Yliniemi, M. Illikainen, Mechanical transformation of phyllite mineralogy toward its use as alkali-activated binder precursor, Miner. Eng. 145 (2020), 106093, https://doi.org/10.1016/j.mineng.2019.106093.
[106] M.H. Samarakoon, P.G. Ranjith, V.R.S. De Silva, Effect of soda-lime glass powder on alkali-activated binders: rheology, strength and microstructure characterization, Constr. Build. Mater. 241 (2020), 118013, https://doi.org/10.1016/j.conbuildmat.2020.118013.
[107] R. Xiao, Y. Zhang, X. Jiang, P. Polaczyk, Y. Ma, B. Huang, Alkali-activated slag supplemented with waste glass powder: laboratory characterization, thermodynamic modelling and sustainability analysis, J. Clean. Prod. 286 (2021), 125554, https://doi.org/10.1016/j.jclepro.2020.125554.
[108] V. Nikolić, M. Komljenović, N. Marjanović, Z. Baščarević, R. Petrović, Lead immobilization by geopolymers based on mechanically activated fly ash, Ceram. Int. 40 (2014) 8479–8488, https://doi.org/10.1016/j.ceramint.2014.01.059.
[109] H. Zhu, M. Zhai, G. Liang, H. Li, Q. Wu, C. Zhang, S. Hua, Experimental study on the freezing resistance and microstructure of alkali-activated slag in the presence of rice husk ash, J. Build. Eng. 38 (2021), 102173, https://doi.org/10.1016/j.jobe.2021.102173.
[110] A. Vásquez, V. Cárdenas, R.A. Robayo, R.M. de Gutiérrez, Geopolymer based on concrete demolition waste, Adv. Powder Technol. 27 (2016) 1173–1179, https://doi.org/10.1016/j.apt.2016.03.029.
[111] R.M. Novais, G. Ascensão, M.P. Seabra, J.A. Labrincha, Waste glass from end-of-life fluorescent lamps as raw material in geopolymers, Waste Manag 52 (2016) 245–255, https://doi.org/10.1016/j.wasman.2016.04.003.